

Threshold behaviour of scattering poles

Eef van Beveren

Centro de Física Teórica

Departamento de Física, Universidade de Coimbra

P-3004-516 Coimbra, Portugal

eef@teor.fis.uc.pt

George Rupp

Centro de Física das Interações Fundamentais

Instituto Superior Técnico, Edifício Ciência

P-1049-001 Lisboa Codex, Portugal

george@ajax.ist.utl.pt

PACS number(s): 11.80.Et, 12.40.Yx, 13.75.Lb, 14.40.-n

Talk given at the

High-Energy Physics Workshop

Scalar Mesons: an Interesting Puzzle for QCD

May 16 - 18, 2003

SUNY Institute of Technology, Utica (NY)

hep-ph/0306185

March 25, 2022

Abstract

The results of a model for meson-meson scattering are studied. The model is shown to be capable of on the one hand reproducing the scattering data, while on the other hand a quark-antiquark confinement spectrum can be determined.

It is concluded that adopting the model's formulation of the transition matrix elements for data analysis, it may serve as a link between experiment and quenched lattice calculations.

1 Introduction

In the sixties, early seventies, mesons and baryons were studied in terms of models for confinement of the newly invented quarks [1,2]. The basic idea was that mesons and baryons could be described

by permanently confined quarks and/or antiquarks. In Fig. (1a) we give an artist's impression of the resulting mass spectrum for mesons.

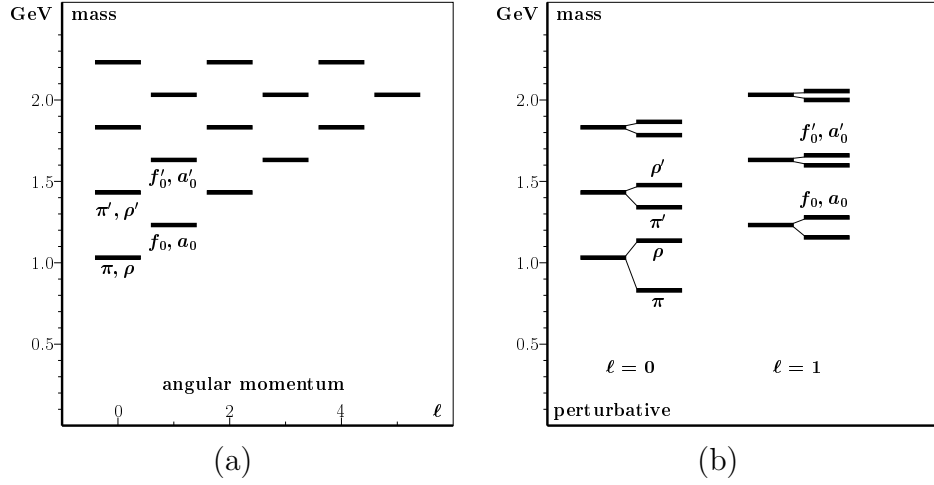


Figure 1: Mass spectrum for a permanently closed system without (a), and including short distance effects perturbatively (b). The parameters are taken from Ref. [3], where harmonic-oscillator confinement is employed.

Then, in the seventies, early eighties, short-range effects had to overcome the small disagreements between Nature and confinement models, as schematically depicted in Fig. (1b). Later, hadronic decay was implemented, with effects on the meson masses as shown in Fig. 2.

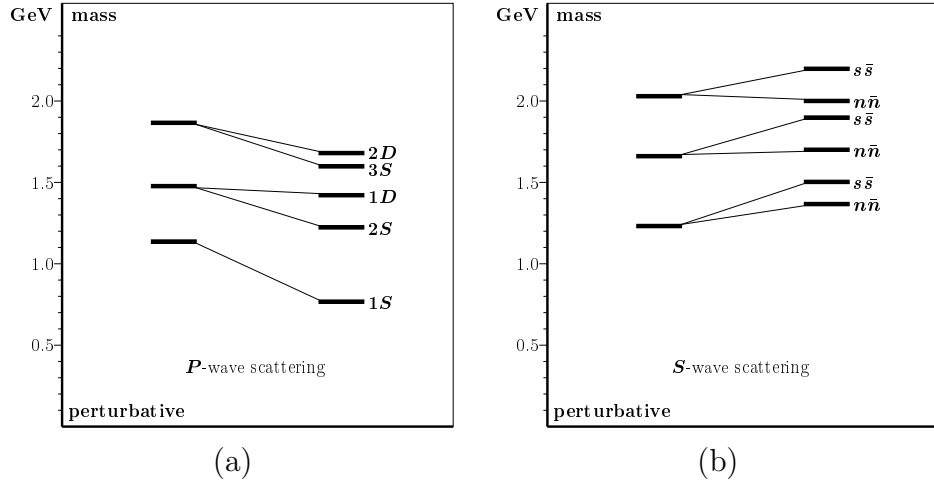


Figure 2: Mass splittings for a permanently closed system when hadronic decay is perturbatively taken into account, for P wave (a), and for S wave (b).

However, it was all the time overlooked how those mesons are actually produced in experiment. In particular, it was taken for granted that mesonic states below a particular meson-meson threshold do not feel the presence of that two-meson channel. Effects of coupling were assumed

to abruptly vanish or show up, depending on whether the state was just above or just below threshold. For states far below threshold, the whole idea of implementing two-meson channels in the confinement models was considered inopportune. Furthermore, little attention was paid to the fact that most mesons appear as resonances, and that mesonic resonance widths are usually not small. For example, a ρ meson has a lifetime compatible with its internal frequency, implying that it should certainly not be considered a more or less stable particle. Even nowadays this is not fully accepted or even understood.

The procedure that mimics the experimental situation is called *unitarization* at present. This name suggests that all is accounted for, which is of course an illusion. In practice, one is more than satisfied if the “most important” effects are included in the resulting meson model.

Also in the seventies one became aware of phenomena in S -wave meson-meson scattering which could not be easily handled by any of the models. Hence, still in the spirit of permanent confinement, quark configurations were invented for mesons and baryons other [4, 5, 6] than the usual $q\bar{q}$ and q^3 .

However, things really fall in place when full scattering properties are determined for meson-meson, or meson-baryon, processes, since then resonances come out automatically without any need to worry about their composition.

We observe the following:

- The higher radial excitations in $c\bar{c}$ and $b\bar{b}$ vector states are almost equally spaced in mass. Why the ground states for those systems come out much lower is well explained [7].
- The level splittings for the S and D $c\bar{c}$ and $b\bar{b}$ vector states follow naturally [7].
- The phase shifts for $K\pi$ and $\pi\pi$ in P wave [3], and in S wave [8], as well as the scattering lengths [9] are reproduced.
- The $J^P = 0^+$ $c\bar{s}$ experimental results are explained [10].
- The $J^P = 1^+$ $c\bar{n}$ (n for nonstrange, either up or down) and $c\bar{s}$ phenomena come out well [11].
- It fully explains the light scalar meson nonet [8].

No extra forces and/or configurations are necessary to explain such an amount of very different data, with one set of parameters for all mesons.

We may thus conclude that unitarization works well. Nevertheless, our model is far from perfect for many reasons that are easy to understand. First, for the transition potential, which

should have been derived from the theory of strong interactions, we make an as simple as possible choice, and then it is still further simplified [12]. Furthermore, also harmonic-oscillator confinement does not have much more justification than the equal-level spacings for $c\bar{c}$ and $b\bar{b}$ (and possibly also $n\bar{n}$ and $s\bar{s}$) vector states. Hence, our choices for both, the confinement and unitarization ingredients, are taken as simple as possible. The fact that it works even under such extreme simplifications clearly indicates that, in a more elaborate approach, the unitarization scheme has a good chance to survive all tests.

2 Unitarization

In order to understand our approach to unitarization, one may imagine a huge scattering or transition matrix, describing all possible scattering of meson pairs. Elastic processes appear on its diagonal, whereas off-diagonal matrix elements describe inelastic processes. Conservation laws predict that the vast majority of off-diagonal matrix elements vanish. The remaining nonvanishing matrix elements can be regrouped into smaller submatrices of meson-meson channels which under the given conservation laws are allowed to communicate. Hence, if we for example study the $J^P = 0^+ c\bar{s}$ system, then we consider the part of the T matrix which describes the S -wave scattering of all meson pairs that through OZI-allowed processes couple to $c\bar{s}$. In practice, we limit ourselves to a few channels which we “believe” are relevant to the energy domain under study. In the following we shall concentrate on just one scattering channel. But the results are equally valid when more channels are taken into account.

Let us now consider an arbitrary diagonal element of the above-discussed transition matrix in a specific partial wave, which we denote by T_ℓ . It describes the elastic scattering of two mesons, assumed not to couple to anything else but the confinement system having the corresponding quantum numbers. We assume here that confinement yields an infinite spectrum. The function T_ℓ must be analytic in the total invariant mass $E = \sqrt{s}$ of the two-meson system. Moreover, it depends on the meson masses M_1 and M_2 , the intensity λ of the coupling between the two-meson system and the confined quark-antiquark system, and finally on the confinement spectrum E_n ($n = 0, 1, 2, \dots$) and other details $\mathcal{F}_{q\bar{q}}$ of the $q\bar{q}$ system. In Ref. [12], the interested reader may find a rather general and complete expression for T_ℓ . Summarizing, we conclude

$$T_\ell = T_\ell(\sqrt{s}, \lambda, M_1, M_2; \{E_n \mid n = 0, 1, 2, \dots\}, \dots) \quad . \quad (1)$$

In Fig. 3 we have depicted a possible spectrum for confinement. The spectrum corresponds to $\lambda = 0$, i.e., having discrete energy eigenvalues of the confinement operator under the assumption

that the $q\bar{q}$ system is decoupled from the meson-meson continuum.

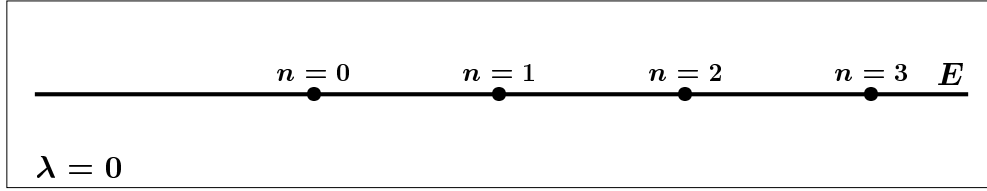


Figure 3: The spectrum of confinement.

When the confinement states are weakly coupled to the meson-meson continuum (λ small), we observe narrow resonances in the two-meson scattering cross section σ , about at the energy eigenvalues of confinement. This is depicted in Fig. 4.

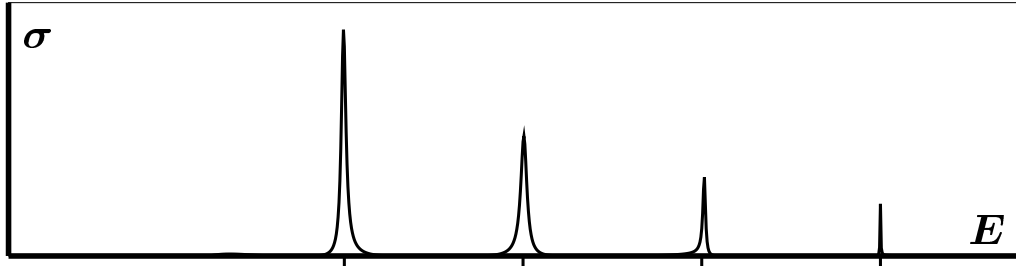


Figure 4: Confinement spectrum as observed in elastic meson-meson scattering, for the case that the confinement states are only weakly coupled to the meson-meson continuum.

The cross section in Fig. 4 is calculated by the use of the transition matrix element T_ℓ of Eq. (1), an explicit expression of which can be found in Ref. [12]. Now, since T_ℓ is an analytic function in the total invariant two-meson mass $E = \sqrt{s}$, one may study its singularity structure for complex E . This can be done numerically. In Fig. 5, we show the poles associated with the resonances in the cross section depicted in Fig. 4.

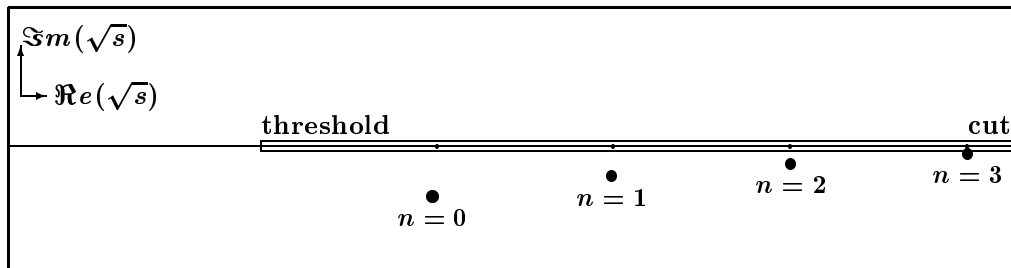


Figure 5: The scattering-matrix poles associated with the resonances shown in Fig. 4. Threshold is at $\sqrt{s} = M_1 + M_2$. The confinement energy eigenvalues are indicated by small dots on the real-energy axis.

The real parts of the poles are close to the energy eigenvalues of the confinement spectrum, while the imaginary parts are relatively small as the resonances are narrow.

In the following we study how the scattering-matrix poles move through the complex-energy plane, when the coupling λ between the meson-meson and confinement systems is increased, in particular near threshold.

But first, let us discuss how a pole of the scattering matrix behaves when the confinement spectrum ($\lambda = 0$) has a state which is below threshold. In our model, these poles shift to even lower energies when λ is increased [7], but remain on the real-energy axis. Such poles correspond to bound states of the coupled system. In this case, both the two-meson and the $q\bar{q}$ components of the wave function describe bound systems. The corresponding states are thus mixtures of bound two-meson and $q\bar{q}$ states.

3 Behavior at threshold

When the ground state of the confinement spectrum is near a non- S -wave threshold, then the associated T -matrix pole passes through threshold when λ is increased [11]. This phenomenon is depicted in Fig. 6.

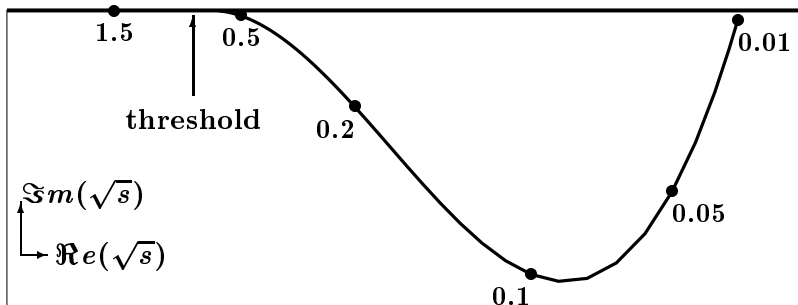


Figure 6: Scattering-matrix pole position of the ground-state resonance, as a function of the coupling constant λ , for P - and higher-wave scattering. Some values of λ are indicated along the curve.

We observe that, while the real part of the pole is continuously decreasing when λ is increased, the imaginary part first increases (in modulus), then decreases, vanishes right at threshold, and remains zero when λ is still further increased. For small values of λ , the displacements of the scattering-matrix poles in the complex-energy plane are almost perturbative, i.e., linear in λ^2 . However, when λ grows it becomes clear that the model incorporates highly nonperturbative effects.

The pole displacement depicted in Fig 6 represents two-meson scattering in P wave. For higher waves the behavior is similar. This can easily be understood by studying the effective-

range expansion near threshold. For P wave and higher waves, one finds that the imaginary part of the pole is quadratic in λ when the real part of the linear momentum is small, which is near threshold. Consequently, at threshold it vanishes.

However, S -wave poles behave very differently [13, 14]. They approach the real-energy axis perpendicularly well below threshold for increasing λ . Then, for still larger values of λ , they first move in the positive direction towards threshold, as virtual bound states. At threshold they turn back, now moving towards smaller energies as genuine bound states. This can more easily be understood from their movement in the complex-linear-momentum plane [15, 13]. Experimentally, one can determine whether the pole represents a virtual or a real bound state from the sign of the scattering length.

4 Poles from the quark-pair-creation cavity

For small coupling, it is very clear how poles in the scattering amplitude are related to the energy eigenvalues of confinement, since their displacements are perturbative, hence small. However, for strong coupling pole displacements can be of the order of magnitude of the level splittings of the confinement spectrum. In this case the situation is more complicated, and were it not for a model to trace the poles, the classification in terms of a confinement spectrum might turn impossible.

But there is more: even when all poles are traced, starting from the small- λ positions near the confinement spectrum, and ending up at the physical positions fitting the scattering data, there exist still more poles in the complex-energy plane. This means that the scattering amplitude which agrees with experiment contains more poles than just those stemming from the confinement spectrum. But let us first discuss where such *extra* poles happen to originate in the model.

In our model, the two-meson system communicates with the confined $q\bar{q}$ system through OZI-allowed quark-pair creation. The shape of the corresponding potential has a maximum at relatively large distances (0.5–1.0 fm). This means that in the interior one has a small potential well which in principle could host bound states. For small coupling, the well is almost flat and thus of no consequence, giving rise to merely mathematical poles with very large negative imaginary parts, hence unobservable. However, for strong coupling these *cavity poles* will turn out to get mixed up with the poles originating in the confinement spectrum. In such a case, there are clearly observable effects in the scattering cross section. Under certain conditions, the poles even end up on the real-energy axis as bound states. In the past we referred to these poles as *background* poles, since for decreasing coupling they disappear into the background. Here, we shall stick to the term *extra* poles.

The extra poles were first reported in Ref. [8]. Later, it was thought that they were the result

of pole doubling [16], a term which we adopted for a while. But now it has become clear from which mechanism they originate.

For meson-meson scattering in S wave, it is more likely that certain structures in the cross section stem from the *extra* poles than for P and higher waves. The reason is that in S -wave scattering the centrifugal barrier is absent. Consequently, the transition-potential well is deeper in the latter case. This is exactly what is observed in experiment.

There are several parameters influencing the displacements of the extra poles, one of them being the relative position of threshold with respect to the confinement spectrum. When threshold is far below the confinement-spectrum ground state, which is usually the case when pions are involved, then the extra pole does not come close to the real-energy axis, causing a broad structure in the scattering cross section, which often is not even a clear resonance. When threshold is closer to the confinement-spectrum ground state, then the extra pole comes closer to the real-energy axis, but the real part of the pole position is below threshold, causing structure at threshold. When threshold is sufficiently close to the confinement-spectrum ground state, then the extra poles end up on the real-energy axis below threshold, where they give rise to bound states, or possibly virtual bound states close to threshold. In Fig. 7 we show the various possibilities.

In order to study the pole displacements as a function of the coupling, we normalize λ such that $\lambda = 1$ corresponds to the physical situation in Fig. 7. The confinement spectrum is chosen to have a ground state at 1.3 GeV and a level spacing of 0.4 GeV. We study meson-meson scattering in S wave. One of the two mesons has a fixed mass of 0.5 GeV, the other is varied in order to obtain different values for threshold. A first observation from Fig. 7 is that the extra pole resides at minus infinity imaginary energy when the meson-meson system is uncoupled from the confinement states.

From Fig. 7a, where the second meson mass is equal to 0.2 GeV, so threshold is at 0.7 GeV, we observe that the extra pole comes out at $(0.711 - i0.20)$ GeV for $\lambda = 1$. In the cross section this gives rise to a very broad resonance-like structure.

In Fig. 7b we choose 0.31 GeV for the second meson mass, so threshold lies at 0.81 GeV. In this case we find the physical pole on the real-energy axis, some 73 MeV below threshold, but still before having reached threshold. Such a pole represents a virtual bound state, which reflects itself in some structure at threshold in the scattering cross section. Only for $\lambda = 1.2$ the pole arrives at threshold. Notice also that the pole reaches the real-energy axis at 0.70 GeV, which is 110 MeV below threshold. Such a phenomenon only occurs for S -wave scattering.

In Fig. 7c the second meson mass equals 0.48 GeV, which brings threshold to 0.98 GeV. The situation near threshold is now more confusing, but we have enlarged that part of the figure in

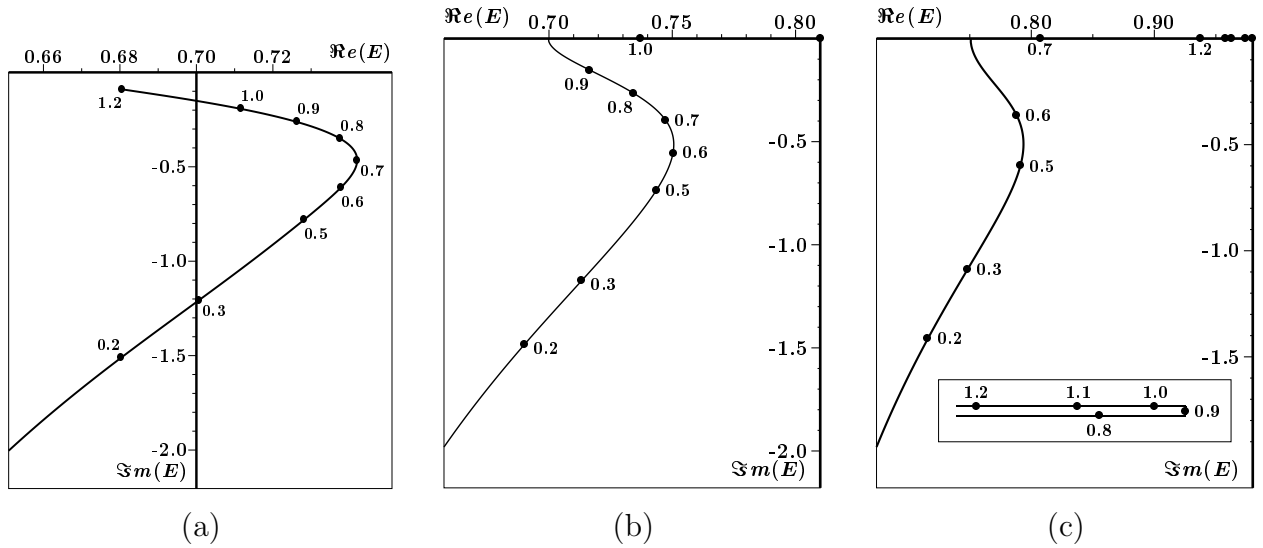


Figure 7: The extra poles w.r.t. threshold.

the inset. From the inset of Fig. 7c we learn that the physical pole comes out some 10 MeV below threshold, but this time as a real bound state. Note that in this case the pole arrives at the real axis 230 MeV below threshold.

In the next section we discuss well-known experimental facts supporting the existence of extra poles in the scattering amplitude for strong interactions.

5 The scalar mesons

As extra poles show up mainly in S -wave scattering, it has to be expected that scalar mesonic resonances must be the domain to search for them [8].

For $K\pi$ and $\pi\pi$ scattering, threshold is far below the ground states of the respective confinement spectra $u\bar{s}$ and $(u\bar{u} + d\bar{d})/\sqrt{2}$, which are at 1.389 GeV resp. 1.287 GeV in our model with the parameters of [3]. This is the situation comparable to Fig. 7a. Consequently, the poles associated with the $K_0^*(791)$ and the $f_0(400-600)$ resonances are still deep in the second Riemann sheet, causing broad structures in the scattering cross sections. In Ref. [8], the respective poles were found at $(727 - i 263)$ MeV and $(470 - i 208)$ MeV, well explaining the scattering data.

The $K\bar{K}$ threshold at some 0.99 GeV is much closer to the $s\bar{s}$ and $(u\bar{u} - d\bar{d})/\sqrt{2}$ ground states at 1.491 GeV and 1.287 GeV. The poles end up just below threshold, as bound states of the coupled systems [14, 17]. But $s\bar{s}$ also couples to $\pi\pi$ in our many-channel model [8], through the chain

$$s\bar{s} \longrightarrow K\bar{K} \longrightarrow \frac{1}{\sqrt{2}} (u\bar{u} + d\bar{d}) \longrightarrow \pi\pi \quad , \quad (2)$$

whereas $(u\bar{u} - d\bar{d})/\sqrt{2}$ also couples to $\pi\eta$.

The $s\bar{s}$ channel couples to $\pi\pi$ through the chain (2), implying that the effective coupling is small [18, 19]. Hence, the resulting pole displacement relative to the mentioned bound state below threshold, is small. In [8] one finds $(994 - i 20)$ MeV for this pole, associated to the $f_0(980)$ resonance.

In the case of the $a_0(980)$ resonance, both $K\bar{K}$ and $\pi\eta$ couple directly, through OZI-allowed pair creation/annihilation, to $(u\bar{u} - d\bar{d})/\sqrt{2}$. However, the coupling intensity for $\pi\eta$ is three times smaller than for $K\bar{K}$. Consequently, we may deal with $\pi\eta$ as a perturbative correction to $K\bar{K}$ here, resulting in an additional shift of the pole in the negative-imaginary direction in the complex-energy plane. In the full multi-channel calculation of Ref. [8], the pole corresponding to the $a_0(980)$ was obtained at $(968 - i 28)$ MeV.

6 The model's K matrix

In its one but simplest form, the model's K matrix for low-energy elastic meson-meson scattering in ℓ wave is given by the expression

$$K_\ell(p) = \frac{2a^4\lambda^2\mu p j_\ell^2(pa) \sum_{n=0}^{\infty} \frac{|\mathcal{F}_{n\ell_c}(a)|^2}{E(p) - E_{n\ell_c}}}{2a^4\lambda^2\mu p j_\ell(pa) n_\ell(pa) \sum_{n=0}^{\infty} \frac{|\mathcal{F}_{n\ell_c}(a)|^2}{E(p) - E_{n\ell_c}} - 1} \quad . \quad (3)$$

In formula (3), p , μ , and $E(p)$ respectively represent the linear momentum, reduced mass, and total invariant mass of the two-meson system. Furthermore, a stands for the average distance where quark-pair creation/annihilation takes place, $\mathcal{F}_{n\ell_c}$ is the radial part of the eigensolution of the confinement system with radial excitation n in ℓ_c wave and for eigenvalue $E_{n\ell_c}$, j_ℓ and n_ℓ are the spherical Bessel resp. Neumann functions, and λ represents the coupling between the two-meson and the confinement systems. In Ref. [12] we give a derivation of formula (3).

One easily deduces for small λ , assuming there exists a pole close to one of the confinement energy eigenvalues, say $E_{\nu\ell_c}$, that the pole displacement, defined by

$$\Delta_{\nu\ell_c} = E - E_{\nu\ell_c} \quad ,$$

is given by the relation

$$\Delta_{\nu\ell_c} \approx 2a^4\lambda^2\mu p^{(\nu)} j_\ell(p^{(\nu)}a) \left[n_\ell(p^{(\nu)}a) - i j_\ell(p^{(\nu)}a) \right] |\mathcal{F}_{\nu\ell_c}(a)|^2, \quad (4)$$

where $p^{(\nu)}$ is the linear momentum corresponding to the energy $E_{\nu\ell_c}$.

Notice from relation (4) that the imaginary part of the pole displacement is negative, as it should be when $E_{\nu\ell_c}$ is above threshold.

It should also be clear at this stage that, by letting λ increase, one may follow the pole's trajectory, but when next λ is decreased, the pole nicely returns to $E_{\nu\ell_c}$. Hence, the extra poles do not show up this way.

In the other limit of very large λ , one ends up with a very simple relation for the pole positions, namely

$$j_\ell(pa) + i n_\ell(pa) = 0, \quad (5)$$

which is the relation for infinite-hard-sphere scattering in ℓ wave.

For data analysis of meson-meson scattering data, the form of the K matrix in Eq. (3) is as good as any Breit-Wigner expansion. But it has two advantages:

- It automatically incorporates the extra poles, without any additional parameter.
- In the limit $\lambda \downarrow 0$, one obtains the confinement spectrum, equivalent to quenched-lattice spectra.

In real data analysis, one may just take a few terms of the summation over the radial quantum number n , and approximate the rest of the summation by a constant. Since, furthermore, confinement is not understood, the moduli squared of the eigenstates $|\mathcal{F}_{n\ell_c}(a)|^2$ and the eigenvalues $E_{n\ell_c}$ turn into fit parameters for data analysis, to be adjusted to experiment. The resulting *experimentally* determined confinement spectrum must coincide with the quenched-lattice spectra. This moreover implies that the light scalars are no issue for quenched-lattice calculations. Thus, a perfect mediator between experiment and low-energy QCD is created through expression (3).

Finally, note that the expression (3) could as well serve for baryon-meson [20] or baryon-antibaryon scattering.

7 Conclusions

Through unitarization, transition matrices can be constructed describing meson-meson scattering. Here we discussed a method which reproduces low-energy data for those two-meson systems

that couple through OZI-allowed processes to nonexotic confined states. By studying its pole structure, we discovered that there exist two types of singularities in the scattering amplitude when analytically continued to complex energies. One type of poles can be directly related to the confinement spectrum, even for cases where pole displacements are large. In the limit of large coupling, these poles are equivalent to scattering from a hard sphere. Poles of the other type stem from the background, and are mainly important for scattering in S wave, the light scalar mesons being their most important manifestation, as well as the recently observed *BABAR* [21] resonance [10, 12].

When applied in data analysis, the model's K matrix might build the bridge between experiment and QCD lattice calculations.

Acknowledgments: One of us (EvB) wishes to thank the organizers of the Scalar Mesons Workshop for kindly inviting him and for their warm hospitality. It was a pleasure to be hosted at the beautiful surroundings and facilities of SUNY Institute of Technology at Utica, New York. He, moreover, thanks Carla Göbel, Sandra Malvezzi, Luigi Moroni, Brian Meadows, Ignácio Bediaga, and Robert Jaffe for useful suggestions for future work. This work was partly supported by the *Fundação para a Ciência e a Tecnologia* of the *Ministério da Ciência e da Tecnologia* of Portugal, under contract number POCTI/FNU/49555/2002.

References

- [1] G. Zweig, CERN Reports TH-401 and TH-412, see also *Developments in the Quark Theory of Hadrons*, Vol. 1, pp. 22–101 (1981), edited by D. B. Lichtenberg and S. P. Rosen.
- [2] Murray Gell-Mann, Phys. Rev. **125**, 1067 (1962).
- [3] E. van Beveren, G. Rupp, T. A. Rijken, and C. Dullemond, Phys. Rev. D **27**, 1527 (1983).
- [4] Robert L. Jaffe, Phys. Rev. D **15**, 267 (1977).
- [5] A. T. Aerts, P. J. Mulders, and J. J. De Swart, Phys. Rev. D **21**, 1370 (1980).
- [6] P. J. Mulders, A. T. Aerts, and J. J. De Swart, Phys. Rev. D **21**, 2653 (1980).
- [7] E. van Beveren, C. Dullemond, and G. Rupp, Phys. Rev. D **21**, 772 (1980) [Erratum-ibid. D **22**, 787 (1980)].
- [8] E. van Beveren, T. A. Rijken, K. Metzger, C. Dullemond, G. Rupp, and J. E. Ribeiro, Z. Phys. C **30**, 615 (1986).

- [9] Eef van Beveren and George Rupp, Eur. Phys. J. C **22**, 493 (2001) [arXiv:hep-ex/0106077].
- [10] Eef van Beveren and George Rupp, arXiv:hep-ph/0305035, to appear in Phys. Rev. Lett. (2003).
- [11] E. van Beveren and G. Rupp, arXiv:hep-ph/0306051.
- [12] Eef van Beveren and George Rupp, Talk given at *The 25th annual Montreal-Rochester-Syracuse-Toronto Conference on High-Energy Physics*, Joefest, *in the honor of the 65th birthday of Joseph Schechter, May 13 - 15, 2003, Syracuse (NY)*, to appear in AIP Conf. Proc. (2003), arXiv:hep-ph/0306155.
- [13] Eef van Beveren, George Rupp, Nicholas Petropoulos, and Frieder Kleefeld, AIP Conf. Proc. **660**, 353 (2003) [arXiv:hep-ph/0211411].
- [14] E. van Beveren and G. Rupp, Int. J. Theor. Phys. Group Theor. Nonlin. Opt., in press (2003) [arXiv:hep-ph/0304105].
- [15] E. Van Beveren, T. A. Rijken, C. Dullemond, and G. Rupp, Lect. Notes Phys. **211**, 331 (1984).
- [16] Nils A. Törnqvist, Z. Phys. C **68**, 647 (1995) [arXiv:hep-ph/9504372].
- [17] Eef van Beveren and George Rupp, Contributed to 31st International Conference on High Energy Physics (ICHEP 2002), Amsterdam, The Netherlands, 24–31 Jul 2002, arXiv:hep-ph/0207022.
- [18] P. Colangelo and F. De Fazio, Phys. Lett. B **559**, 49 (2003) [arXiv:hep-ph/0301267].
- [19] F. De Fazio and M. R. Pennington, Phys. Lett. B **521**, 15 (2001) [arXiv:hep-ph/0104289].
- [20] J. Ellis, Y. Frishman, and M. Karliner, arXiv:hep-ph/0305292.
- [21] B. Aubert *et al.* [BABAR Collaboration], arXiv:hep-ex/0304021, to appear in Phys. Rev. Lett. (2003).